Analysis of Exchange Interaction and Electron Delocalization as Intramolecular Determinants of Intermolecular Electron-Transfer Kinetics

E. L. Bominaar,*,† C. Achim,† S. A. Borshch,‡ J.-J. Girerd,§ and E. Münck†

Department of Chemistry, Carnegie Mellon University, Pittsburgh, Pennsylvania 15213, Institut de Recherches sur la Catalyse, CNRS, 69626 Villeurbanne cedex, France, and Laboratoire de Chimie Inorganique, URA CNRS 420, Université de Paris-Sud, 91405 Orsay, France

Received October 25, 1996[⊗]

During the past decades, spectroscopic characterization of exchange interactions and electron delocalization has developed into a powerful tool for the recognition of metal clusters in metalloproteins. By contrast, the biological relevance of these interactions has received little attention thus far. This paper presents a theoretical study in which this problem is addressed. The rate constant for intermolecular electron-transfer reactions which are essential in many biological processes is investigated. An expression is derived for the dependence of the rate constant for self-exchange on the delocalization degree of the mixed-valence species. This result allows us to rationalize published kinetic data. In the simplest case of electron transfer from an exchange-coupled binuclear mixed-valence donor to a diamagnetic acceptor, the rate constant is evaluated, taking into account spin factors and exchange energies in the initial and final state. The theoretical analysis indicates that *intra*molecular spin-dependent electron delocalization (double exchange) and Heisenberg−Dirac−van Vleck (HDvV) exchange have an important impact on the rate constant for *inter*molecular electron transfer. This correlation reveals a novel relationship between magnetochemistry and electrochemistry. Contributions to the electron transfer from the ground and excited states of the exchange-coupled dimer have been evaluated. For clusters in which these states have different degrees of delocalization, the excited-state contributions to electron transfer may become dominant at potentials which are less reductive than the potential at which the rate constant for the transfer from the ground state is maximum. The rate constant shows a steep dependence on HDvV exchange, which suggests that an exchange-coupled cluster can act as a molecular switch for exchange-controlled electron gating. The relevance of this result is discussed in the context of substrate specificity of electron-transfer reactions in biology. Our theoretical analysis points toward a possible biological role of the spin-state variability in iron−sulfur clusters depending on cluster environment.

1. Introduction

Electron transfer in biological systems makes extensive use of metalloproteins.[1,2] The metal centers act as redox sites in the consecutive stages of biological electron-transfer reactions which constitute the basis of many vital processes such as respiration and photosynthesis.[3] These electron carriers include mononuclear sites as well as polynuclear clusters. Mononuclear sites based on Fe are found in cytochromes and rubredoxins.[4−8] Polynuclear clusters comprise the redox centers in iron−sulfur proteins,[8−10] iron−oxo proteins such as methane monooxygenase and ribonucleotide reductase,[11] and the Mn water-oxidation catalyst of photosystem II.[12] Recent X-ray studies of cytochrome *c* oxidase have conclusively proved that the Cu_A unit in this protein is a binuclear cluster,[13,14] confirming an early structure prediction based on EPR spectroscopy.[15] In redox reactions, the clusters may attain heterovalent oxidation states which are referred to as mixed-valence states.[16,17]

Factors determining the kinetics of electron transfer in biological systems are the subject of continuing interest. Comprehensive reviews on different aspects of electron transfer are found in refs 1, 2, and 18−20. The rate constant for a nonadiabatic electron-transfer reaction can be expressed as *k*

† Carnegie Mellon University.
‡ Institut de Recherches sur la Catalyse.
§ Université de Paris-Sud.
⊗ Abstract published in *Advance ACS Abstracts,* August 1, 1997.

(1) Johnson, M. K.; King, R. B.; Kurtz, D. M.; Kutal, C.; Norton, M. L.; Scott, R. A. *Electron Transfer in Biology and the Solid State*; American Chemical Society: Washington, DC, 1990; Vol. 226.
(2) Bolton, J. R.; Mataga, N.; McLendon, G. *Electron Transfer in Inorganic, Organic, and Biological Systems*; American Chemical Society: Washington, DC, 1991; Vol. 228.
(3) Lippard, S. J.; Berg, J. M. *Principles of Bioinorganic Chemistry*; University Science Books: Mill Valley, CA, 1994.
(4) Moore, G. R.; Pettigrew, G. W. *Cytochromes C*; Springer-Verlag: New York, 1990.
(5) Babcock, G. T.; Wikström, M. *Nature* **1992**, *356*, 301−309.
(6) Evans, M. C. W. In *Iron−Sulfur Proteins*; Spiro, T. G., Ed.; Wiley-Interscience Publication: New York, 1982.
(7) Ohnishi, T.; Salerno, J. C. In *Iron−Sulfur Proteins*; Spiro, T. G., Ed.; Wiley-Interscience Publication: New York, 1982.
(8) Cammack, R. *Iron−Sulfur Proteins*; Academic Press, Inc.: San Diego, CA, 1992; Vol. 38.
(9) Karlin, K. D.; Tyeklár, Z. *Bioinorganic Chemistry of Copper*; Chapman and Hall Inc.: New York, 1993.
(10) Solomon, E. I. In *Metal Clusters in Proteins*; Que, L., Ed.; American Chemical Society: Washington, DC, 1988; Vol. 372, pp 116−150.
(11) Que, L.; True, A. E. *Prog. Inorg. Chem.* **1990**, *38*, 97−200.
(12) Pecoraro, V. L. *Manganese Redox Enzymes*; VHC Publishers: New York, 1992.
(13) Tsukihara, T.; Aoyama, H.; Yamashita, E.; Tomizaki, T.; Yamaguchi, H.; Shizawa-Itoh, K.; Nakashima, R.; Yaono, R.; Yoshikawa, S. *Science* **1995**, *269*, 1069−1074.
(14) Iwata, S.; Ostermeier, C.; Ludwig, B.; Michel, H. *Nature* **1995**, *376*, 660−669.
(15) Beinert, H.; Griffiths, D. E.; Wharton, D. C.; Sands, R. H. *J. Biol. Chem.* **1962**, *237*, 2337−2346.
(16) Prassides, K. *Mixed Valency Systems: Applications in Chemistry, Physics, and Biology*; Kluwer Academic Publishers: Dordrecht, The Netherlands, 1991.
(17) Hush, N. S. *Prog. Inorg. Chem.* **1967**, *8*, 391−444.
(18) Barbara, P. F.; Meyer, T. J.; Ratner, M. A. *J. Phys. Chem.* **1996**, *100*, 13148−13168.
(19) Mikkelsen, K. V.; Ratner, M. A. *Chem. Rev.* **1987**, *87*, 113−153.
(20) Marcus, R. A.; Sutin, N. *Biochim. Biophys. Acta* **1985**, *811*, 265−322.

S0020-1669(96)01298-0 CCC: $14.00

$= \pi^{1/2}\hbar^{-1}H_{DA}^2(\chi k_B T)^{-1/2} \exp(-\Delta G^*/k_B T)$, where $\Delta G^* = (\chi + \Delta G^\circ)^2/4\chi$ is the free energy of activation, χ is the reorganization parameter, ΔG° is the free-energy change for the electron-transfer reaction, and H_{DA} is the electronic coupling matrix element.[21] χ contains contributions from changes in inner-sphere bond distances and angles and from outer-sphere polarization of the surrounding dielectric medium, $\chi = \chi_{in} + \chi_{out}$.[17] The inner-sphere contributions are determined by the bonding properties of the donor and acceptor orbitals and are minimized in orbital arrangements for which the transferring electron migrates over nonbonding orbitals.[22] In systems with close-lying orbital states, the reorganization energy may contain important contributions from Jahn−Teller distortions.[23,24] The expression for k implies that a combination of small reorganization energy and large electronic coupling creates favorable conditions for electron transfer. Detailed electronic-structure analysis of the blue copper center in plastocyanin indicates that the metal binding site is specially designed to maximize H_{DA} through optimization of the directionality of the donor orbital.[25] The protein structure as well as the formation of multiprotein complexes and their conformations influences directly the electron pathways and affects the H_{DA} values. Gating by conformational interconversion has been proposed as an explanation for the multiphasic kinetics within the dynamic complex between cytochrome *c* and cytochrome *c* peroxidase.[26−29] Tunneling-path studies of interprotein electron transfer indicate that diprotein complexes which are optimal for electron-transfer reaction require good "contacts" between "conductive" surface patches and do not necessarily optimize the electrostatic interactions between the proteins.[30] In metalloproteins, H_{DA} appears to decrease exponentially as a function of increasing separation between the redox centers.[31] Beside these factors, the effect of exchange interaction on redox potentials was examined by Bertrand and Gayda for 2-Fe ferredoxins.[32] The relevance of spin-dependent resonance interaction for the electrochemical properties of mixed-valence clusters was recognized by Girerd.[33] Noodleman and collaborators analyzed the effect of these interactions on the redox potentials of Fe−S clusters embedded in a continuum dielectric.[34] Bersuker and Borshch predicted that the rate constants for intramolecular electron transfer depend significantly on cluster spin.[35]

Synthetic model compounds afford the study of cluster properties in a nonprotein environment.[36−38] Measurements of ^{1}H NMR line shape changes originating from self-exchange reactions in $[Fe_4S_4(SR)_4]^{3-}/[Fe_4S_4(SR)_4]^{2-}$ mixtures have revealed large rate constants, consistent with a small cluster reorganization energy.[38] Because the intrinsic rates are fast, the electron transfer in proteins can be tuned by factors extrinsic to the cluster. In all known cases, much slower rates than for synthetic clusters are found for electron transfer from protein-bound clusters,[39−41] probably due to a reduction of H_{DA} as a result of a larger donor−acceptor separation. In anticipation of our results, it should be noted that a fast intrinsic electron-transfer rate does not exclude the possibility that Fe−S clusters are an active part of the molecular mechanism controlling electron transfer in biological systems.

Spectroscopic studies have provided detailed insight in the similarities and the differences in the electronic structure of clusters in proteins and synthetic analogs.[42−44] In many respects, the major electronic characteristics remain unchanged when the clusters are placed in a protein environment. Conspicuous electronic features revealed by Mössbauer studies on tri- and tetranuclear mixed-valent Fe−S clusters in both proteins and synthetic analogs are the delocalization of an "extra" electron over two metal sites of the cluster and the concomitant ordering of the Fe spins in $S \approx {}^9/_2$ delocalized $[Fe^{2.5+}Fe^{2.5+}]$ pairs.[42−44] Theoretical studies have shown that partial electron delocalization and spin state in these clusters can be explained by considering an interplay of double exchange and vibronic coupling.[45−48] The condition for delocalization over multiple metal sites is that the gain in reorganization energy accompanying electron trapping at one site of the cluster is smaller than the gain in resonance energy obtained by delocalization of the extra electron.[49]

Electron delocalization (class III according to Robin and Day classification[50]) has been found in a number of binuclear mixed-valence compounds. For example, the unit $[Cu^{1.5+}Cu^{1.5+}]$ ($S = {}^1/_2$) is found in the oxidized Cu_A site in cytochrome *c* oxidase[15,51] and in the model compound $[(L^{PrdacoS}Cu)_2$-

(21) This expression is based on a description of nuclear motion in semiclassical approximation and is valid for $kT > h\nu$. A full quantum-mechanical treatment is more laborious but may reveal some new pecularities of the electron-transfer characteristics of the systems that we intend to study. However, we believe that the main qualitative conclusions of our study remain valid.

(22) Gebhard, M. S.; Deaton, J. C.; Koch, S. A.; Millar, M.; Solomon, E. I. *J. Am. Chem. Soc.* **1990**, *112*, 2217−2231.
(23) Vekhter, B. G.; Rafalovich, M. L. *Chem. Phys.* **1977**, *21*, 21−25.
(24) LaCroix, L. B.; Shadle, S. E.; Wang, Y.; Averill, B. A.; Hedman, B.; Hodgson, K. O.; Solomon, E. I. *J. Am. Chem. Soc.* **1996**, *118*, 7755−7768.
(25) Solomon, E. I.; Lowery, M. D. *Science* **1993**, *259*, 1575−1581.
(26) Peterson-Kennedy, S. E.; McGourty, J. L.; Hoffman, B. M. *J. Am. Chem. Soc.* **1984**, *106*, 5010−5012.
(27) Peterson-Kennedy, S. E.; McGourty, J. L.; Ho, P. S.; Sutoris, C. J.; Liang, N.; Zemel, H.; Blough, N. V.; Margoliash, E.; Hoffman, B. M. *Coord. Chem. Rev.* **1985**, *64*, 125−133.
(28) Hoffman, B. M.; Ratner, M. A. *J. Am. Chem. Soc.* **1987**, *109*, 6237−6243.
(29) Zhou, J. S.; Nocek, J. M.; DeVan, M. L.; Hoffman, B. M. *Science* **1995**, *269*, 204−207.
(30) Ullmann, G. M.; Kostic, N. M. *J. Am. Chem. Soc.* **1995**, *117*, 4766−4774.
(31) Mayo, S. L.; Ellis, W. R.; Crutchley, R. J.; Gray, H. B. *Science* **1986**, *233*, 948.
(32) Bertrand, P.; Gayda, J.-P. *Biochim. Biophys. Acta* **1982**, *680*, 331−335.
(33) Girerd, J.-J. *J. Chem. Phys.* **1983**, *79*, 1766−1775.
(34) Mouesca, J. M.; Chen, J. L.; Noodleman, L.; Bashford, D.; Case, D. A. *J. Am. Chem. Soc.* **1994**, *116*, 11898−11914.
(35) Bersuker, I. B.; Borshch, S. A. *Adv. Chem. Phys.* **1992**, *LXXXI*, 703−782.
(36) Holm, R. H. In *Iron−Sulfur Proteins*; Cammack, R., Ed.; Academic Press: San Diego, CA, 1992; Vol. 38, pp 1−71.
(37) Houser, R. P.; Young, V. G.; Tolman, W. B. *J. Am. Chem. Soc.* **1996**, *118*, 2101−2102.
(38) Reynolds, J. G.; Coyle, C. L.; Holm, R. H. *J. Am. Chem. Soc.* **1980**, *102*, 4350−4355.
(39) Armstrong, F. A.; Henderson, R. A.; Segal, M. G.; Sykes, A. G. *J. Chem. Soc., Chem. Commun.* **1978**, 1102−1103.
(40) Armstrong, F. A.; Sykes, A. G. *J. Am. Chem. Soc.* **1978**, *100*, 7710−7715.
(41) Armstrong, F. A.; Henderson, R. A.; Sykes, A. G. *J. Am. Chem. Soc.* **1979**, *101*, 6912−6917.
(42) Münck, E.; Papaefthymiou, V.; Surerus, K. K.; Girerd, J.-J.; *ACS Symposium Series 372*; American Chemical Society: Washington, DC, 1988; pp 302−325.
(43) Papaefthymiou, V.; Girerd, J.-J.; Moura, I.; Moura, J. J. G.; Münck, E. *J. Am. Chem. Soc.* **1987**, *109*, 4703−4710.
(44) Middleton, P.; Dickson, D. P. E.; Johnson, C. E.; Rush, J. D. *Eur. J. Biochem.* **1980**, *104*, 289−296.
(45) Borshch, S. A.; Chibotaru, L. F. *Chem. Phys.* **1989**, *135*, 375−380.
(46) Borshch, S. A.; Bominaar, E. L.; Blondin, G.; Girerd, J.-J. *J. Am. Chem. Soc.* **1993**, *115*, 5155−5168.
(47) Borshch, S. A.; Bominaar, E. L.; Girerd, J.-J. *New. J. Chem.* **1993**, *17*, 39−42.
(48) Bominaar, E. L.; Borshch, S. A.; Girerd, J.-J. *J. Am. Chem. Soc.* **1994**, *116*, 5362−5372.
(49) This condition does not imply that the trapping forces are weak, since the resonance energies may be big.
(50) Robin, M. B.; Day, P. *Adv. Inorg. Chem. Radiochem.* **1967**, *10*, 247−422.
(51) Kroneck, P. M. H.; Antholine, W. E.; Riester, J.; Zumft, W. G. *FEBS Lett.* **1988**, *242*, 70−74.

(O_3SCF_3)],[37] the $[Fe^{2.5+}Fe^{2.5+}]$ ($S = {}^9/_2$) motif occurs in $[Fe_2(OH)_3(tmtacn)_2]^{2+}$ and in the $[Fe_2S_2]^+$ cluster of molecular variants of *C. pasteurianum* 2-Fe ferredoxin,[52−56] and $[Fe^{3.5+}Fe^{3.5+}]$ ($S = {}^3/_2$) appears in $[Fe_2O_2(5\text{-Me-TPA})_2]^+$.[57] Because the presence of delocalized electronic states appears to be a common feature of polynuclear clusters, it is of interest to investigate how this property may influence their redox activity.

The studies conducted by Monzyk and Holwerda on the kinetics of the self-exchange reactions in a series of binuclear compounds containing a $[N_4Mn^{3+}O_2Mn^{4+}N_4]^{3+/2+}$ core revealed a remarkable correlation between the rate constant for the *inter*molecular electron-transfer reaction $*[Mn^{4+}Mn^{3+}] + [Mn^{3+}Mn^{3+}] \leftrightarrow *[Mn^{3+}Mn^{3+}] + [Mn^{4+}Mn^{3+}]$ and the degree of *intra*molecular electron delocalization in the mixed-valence (4+,3+) state.[58] Using the differences of metal−ligand bond lengths at the $Mn^{3+/4+}$ sites as an indicator of delocalization class, these authors found a 2 orders-of-magnitude increase in the rate constant in passing from a localized species to a partially delocalized (class II) species. Studies of Hupp and Zhang confirm the existence of a correlation between electron delocalization and kinetics.[59] Holm and collaborators have demonstrated that the activation energy for the reaction $*[Fe_4S_4]^{2+} + [Fe_4S_4]^+ \leftrightarrow *[Fe_4S_4]^+ + [Fe_4S_4]^{2+}$ involving synthetic analogs is small as a result of a simultaneous change of four interplanar Fe−S distances.[38,60] In line with these observations, theoretical studies have shown that the activation barrier for intramolecular electron transfer from a delocalized initial state to a delocalized final state is smaller than for transfer between localized states.[48] Recently, a similar type of reduction of activation energy has been proposed in a study of the binuclear Cu_A site in cytochrome *c* oxidase.[61] A diminished rate constant for electron transfer between Cu_A and heme *a* has been reported for the valence-localized Cu_A center in a mutant as compared to the rate constant for the delocalized Cu_A center in the wild type.[62] The correlation between intramolecular delocalization and intermolecular electron-transfer rate has also been interpreted on the basis of the relationship between the solvation energy of a charged body and its size.[59] Thus, the solvation energy of a sphere carrying the unit charge (e), having radius *R*, and merged in a medium with dielectric constant ϵ is given by Born's expression $-(e^2/2R)(1 - 1/\epsilon)$ which shows that the solvation energy decreases with increasing radius.[63] Although the solvent is a major determinant of electron-transfer kinetics, it should be borne in mind that Born's expression retains its validity for any spherically symmetric charge distribution within the sphere, the limiting case being for a point charge at the center of the sphere. Hence, for polynuclear metal centers that are burried in a protein or a bulky ligand environment (such that the cluster is small compared to the dimensions of the protein or ligand), the radius *R* should be identified with the extension of the protein or that of the complex rather than with the dimension of the metal cluster over which the delocalization takes place. In such cases, the effect of intramolecular electron delocalization on solvation energy is expected to be small.[64]

In this paper, we examine aspects of *inter*molecular electron transfer specific for reactions involving exchange-coupled mixed-valence clusters. First, a simple theoretical model is developed for describing how *intra*cluster electron delocalization accelerates *inter*cluster electron transfer by reducing the reorganization energy. The proposed model is based on the common observation that the metal−ligand distances depend on the oxidation state of the metal.[65,66] In order to account for the energetics of structural relaxation accompanying the redox process, we introduce a linear coupling term between the electron density, $n_{X,i}$, and an in-phase breathing mode, $q_{X,i}$, of the ligands in the coordination shell of each metal site, *i*, of the cluster, *X*. This treatment allows us to express the dependence of the reorganization energy on delocalization degree. Second, the model is extended to describe the influence of spin on *inter*molecular electron transfer. We consider the example of electron transfer from a binuclear exchange-coupled mixed-valence donor to a diamagnetic acceptor. An expression for the rate constant is derived using an effective Hamiltonian including terms for vibronic coupling, double exchange, and HDvV exchange.[67] The contributions for electron transfer *via* excited spin states are taken into account. Our analysis identifies spin and electron delocalization as important rate-determining factors of intermolecular electron transfer involving metal clusters.

2. Description of the Model

Let us consider the electron-transfer reaction $D_{red} + A_{ox} \rightarrow D_{ox} + A_{red}$, in which an electron is transferred between two metal clusters, termed donor D and acceptor A, with nuclearity N_D and N_A, and let $\{|\varphi_{D,i}\rangle\}$ and $\{|\varphi_{A,i}\rangle\}$ be two sets of orthogonal basis orbitals centered on the sites, labelled by *i*, of donor D and acceptor A, respectively. The molecular states accommodating the extra electron are written as

$$|\psi_D\rangle = c_{D,1}|\varphi_{D,1}\rangle + ... + c_{D,m}|\varphi_{D,m}\rangle \qquad (1a)$$

$$|\psi_A\rangle = c_{A,1}|\varphi_{A,1}\rangle + ... + c_{A,m'}|\varphi_{A,m'}\rangle \qquad (1b)$$

To describe the electron transfer, we allow for variable occupation numbers of the clusters, n_D and n_A, which fulfill the condition of charge conservation, $n_+ = n_D + n_A = 1$. The electronic occupations of the individual metal sites $i = 1, ..., N_X$ are given by $n_{D,i} = n_D c_{D,i}^2$ and $n_{A,i} = n_A c_{A,i}^2$ and fulfill the relations $n_{D,1} + ... + n_{D,m} = n_D$ and $n_{A,1} + ... + n_{A,m'} = n_A$ which follow from normalization conditions of the wave functions in eq 1a,b. The electron densities at the individual

(52) Crouse, B. R.; Meyer, J.; Johnson, M. K. *J. Am. Chem. Soc.* **1995**, *117*, 9612−9613.
(53) Achim, C.; Golinelli, M. P.; Bominaar, E. L.; Meyer, J.; Münck, E. *J. Am. Chem. Soc.* **1996**, *118*, 8168−8169.
(54) Ding, X.-Q.; Bominaar, E. L.; Bill, E.; Winkler, H.; Trautwein, A. X.; Drüeke, S.; Chaudhuri, P.; Wieghardt, K. *J. Chem. Phys.* **1990**, *92*, 178−186.
(55) Gamelin, D. R.; Bominaar, E. L.; Mathonière, C.; Kirk, M. L.; Wieghardt, K.; Girerd, J.-J.; Solomon, E. I. *Inorg. Chem.* **1996**, *35*, 4323−4335.
(56) Gamelin, D. R.; Bominaar, E. L.; Kirk, M. L.; Wieghardt, K.; Solomon, E. I. *J. Am. Chem. Soc.* **1996**, *118*, 8085−8097.
(57) Dong, Y.; Fuji, H.; Hendrich, M.; Leising, R. A.; Pan, G.; Randall, C. R.; Wilkinson, E. C.; Zang, Y.; Que, L.; Fox, B. G.; Kauffmann, K. E.; Münck, E. *J. Am. Chem. Soc.* **1995**, *117*, 2778−2792.
(58) Monzyk, M. M.; Holwerda, R. A. *Inorg. Chem.* **1992**, *31*, 1969−1971.
(59) Hupp, J. T.; Zhang, X. L. *J. Phys. Chem.* **1995**, *99*, 853−855.
(60) Laskowski, E. J.; Reynolds, J. G.; Frankel, R. B.; Foner, S.; Papaefthymiou, G. C.; Holm, R. H. *J. Am. Chem. Soc.* **1979**, *101*, 6562−6570.
(61) Larsson, S.; Källebring, B.; Wittung, P.; Malmström, B. G. *Proc. Natl. Acad. Sci. U.S.A.* **1995**, *92*, 7167−7171.
(62) Zickermann, V.; Verkhovsky, M.; Morgan, J.; Wikstrom, M.; Annemüller, S.; Bill, E.; Steffens, G. C. M.; Ludwig, B. *Eur. J. Biochem.* **1995**, *234*, 688−693.
(63) Born, M. *Z. Phys.* **1920**, *1*, 45−48.
(64) Williams, R. J. P. Chapter 1 in *Electron Transfer in Biology and the Solid State*; Johnson, M. K., King, R. B., Kurtz, D. M., Kutal, C., Norton, M. L., Scott, R. A., Eds.; American Chemical Society: Washington, DC, 1990; Vol. 226.
(65) Wong, K. Y.; Schatz, P. N. *Prog. Inorg. Chem.* **1981**, *28*, 369−449.
(66) Blondin, G.; Girerd, J.-J. *Chem. Rev.* **1990**, *90*, 1359−1376.
(67) Anderson, P. W. In *Magnetism*; Rado, G. T., Suhl, H., Eds.; Acad. Press: New York, 1963; Vol. I, pp 25−83.

metal sites are coupled to in-phase breathing modes of their environments.[68] The local breathing mode at metal site i of donor cluster D is denoted as $q_{D,i}$ and the one at site i of acceptor cluster A, as $q_{A,i}$. The linear coupling terms are written as $n_{D,i}\lambda q_{D,i}$ and $n_{A,i}\lambda q_{A,i}$. The parameter λ is the vibronic coupling constant. The energies for clusters D and A, eqs 2a,b, contain

$$E_D = {}^1/_2\kappa({q_{D,1}}^2 + ... + {q_{D,m}}^2) + n_D{c_{D,1}}^2\lambda q_{D,1} + ... + n_D{c_{D,m}}^2\lambda q_{D,m} \quad (2a)$$

$$E_A = {}^1/_2\kappa({q_{A,1}}^2 + ... + {q_{A,m'}}^2) + n_A{c_{A,1}}^2\lambda q_{A,1} + ... + n_A{c_{A,m'}}^2\lambda q_{A,m'} \quad (2b)$$

contributions for restoring forces and vibronic coupling. The former contributions are considered in harmonic approximation. In this paper we make the simplifying approximation that the values of (κ, λ) for all the sites of both donor and acceptor clusters are equal.

The electron-transfer process is actively coupled to the cluster modes given in eqs 3a,b which are composed of in-phase

$$Q_{D,s} = \frac{{c_{D,1}}^2 q_{D,1} + ... + {c_{D,m}}^2 q_{D,m}}{\sqrt{{c_{D,1}}^4 + ... + {c_{D,m}}^4}} \quad (3a)$$

$$Q_{A,s} = \frac{{c_{A,1}}^2 q_{A,1} + ... + {c_{A,m'}}^2 q_{A,m'}}{\sqrt{{c_{A,1}}^4 + ... + {c_{A,m'}}^4}} \quad (3b)$$

superpositions of local vibrations with amplitudes proportional to the local charges. The denominators in eqs 3a,b are normalization constants. After unitary transformations to new sets of coordinates, $\{Q_{D,\alpha}\}$ and $\{Q_{A,\alpha'}\}$, which include $Q_{D,s}$ and $Q_{A,s}$, the sum of the energies given in eqs 2, E_{DA}, can be expressed as

$$E_{DA} = {}^1/_2\kappa(\sum_\alpha {Q_{D,\alpha}}^2 + \sum_{\alpha'} {Q_{A,\alpha'}}^2) + \sqrt{f_D}n_D\lambda Q_{D,s} + \sqrt{f_A}n_A\lambda Q_{A,s} \quad (4a)$$

in which the following definitions have been adopted:

$$f_D = {c_{D,1}}^4 + ... + {c_{D,m}}^4 \quad (4b)$$

$$f_A = {c_{A,1}}^4 + ... + {c_{A,m'}}^4 \quad (4c)$$

The f factors correlate with the degrees of delocalization. Because combinations of the local vibrations that are perpendicular to $Q_{D,s}$ and $Q_{A,s}$ are considered to be inactive, they are taken equal to zero, i.e., $Q_{D,\alpha} = 0$ and $Q_{A,\alpha'} = 0$ for $\alpha,\alpha' \neq s$, which yields[69]

(68) Piepho, S. B.; Krausz, E. R.; Schatz, P. N. *J. Am. Chem. Soc.* **1978**, *100*, 2996−3005.

(69) We have adopted a frozen-state approximation. Thus, the electronic state is taken as it is found in the adiabatic potential minimum (see below) and assumed to be independent of the vibrations away from the minimum. This approximation is valid in the case of strong electronic coupling between the metal sites (full delocalization) and in the case of weak coupling (site trapping). In the intermediate regime, however, vibrations perpendicular to Q_{eff} may alter the electronic wave function. Therefore, these vibrations can change the electronic state energies and become active in the electron transfer. For the sake of clarity, we have chosen the present treatment. An analysis based on anharmonic potentials is in progress.

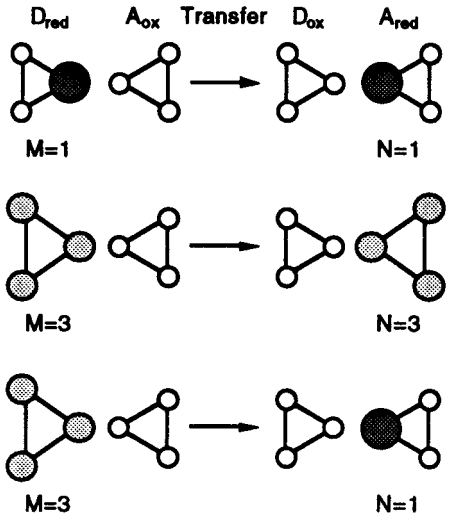

Figure 1. Schematic representation of redox reactions between trinuclear metal clusters. M and N indicate, respectively, the number of metal sites in the mixed-valence clusters D_{red} and A_{red} over which the "transferable" electron is delocalized before and after the reaction. The darkness of the shading depicts the charge density of this electron. The sizes of the circles represent the magnitudes of the distortions in the local coordination shells of the individual metal sites. The first two reactions are between identical species (self-exchange); the reaction at the bottom is between nonidentical species.

$$E_{DA} = {}^1/_2\kappa({Q_{D,s}}^2 + {Q_{A,s}}^2) + \sqrt{f_D}n_D\lambda Q_{D,s} + \sqrt{f_A}n_A\lambda Q_{A,s} \quad (4d)$$

The coordinates $Q_{D,s}$ and $Q_{A,s}$ have been called interaction modes in the literature.[70]

2.1. Activation Energy for Electron Transfer: Identical Sites (Self-Exchange). In the symmetrical case, D and A are identical molecules with identical delocalization patterns. In Figure 1, the top and middle panels depict self-exchange between trinuclear clusters with localized and delocalized valencies, respectively. For the donor−acceptor system, it is convenient to introduce symmetrized vibrations defined as

$$Q_+ = (Q_{D,s} + Q_{A,s})/\sqrt{2} \quad (5a)$$

$$Q_- = (Q_{D,s} - Q_{A,s})/\sqrt{2} \quad (5b)$$

By substitution of eqs 5a,b into eq 4d, the total energy can be expressed as

$$E_{DA} = {}^1/_2\kappa({Q_+}^2 + {Q_-}^2) + \sqrt{f}\left(\frac{n_+\lambda}{\sqrt{2}}Q_+ + \frac{n_-\lambda}{\sqrt{2}}Q_-\right) \quad (6)$$

in which $n_\pm = n_D \pm n_A$ and $f = f_D = f_A$. The total energy (eq 6) is minimum at the following $Q_\pm$ values:

$${Q_+}^{(0)} = -\sqrt{f}\frac{n_+\lambda}{\kappa\sqrt{2}} \quad (7a)$$

$${Q_-}^{(0)} = -\sqrt{f}\frac{n_-\lambda}{\kappa\sqrt{2}} \quad (7b)$$

Because $n_+ = 1$, ${Q_+}^{(0)}$ is independent of charge partitioning over clusters D and A, while ${Q_-}^{(0)}$ depends on electron distribution through n_-. The absolute minima are obtained when

(70) Bersuker, I. B.; Polinger, V. Z. *Vibronic interactions in molecules and crystals*; Springer Verlag: Berlin, 1989; Vol. 49.

the electron is vibronically trapped either on the donor D ($n_- = 1$) or on the acceptor A ($n_- = -1$). The energies of the two "trapped" states at $Q_+^{(0)}$ as a function of the symmetry-breaking coordinate, Q_-, are given by

$$E_{DA} = -f\frac{\lambda^2}{4\kappa} + {}^1/_2\kappa Q_-{}^2 \pm \sqrt{f}\frac{\lambda}{\sqrt{2}}Q_- \quad (8)$$

These energy functions represent two parabola. The height of the energy barrier, ΔG^*, which separates the two well minima is given by

$$\Delta G^*_{c_1,\ldots,c_m} = f\frac{\lambda^2}{4\kappa} \quad (9)$$

The activation energy, eq 9, determines the electron-transfer rate. It follows from eq 9 that the barrier for a donor−acceptor couple in which the extra electron is fully delocalized over N sites, $N \leq N_D = N_A$, is given by

$$\Delta G^*_N = \frac{1}{N}\frac{\lambda^2}{4\kappa} \quad (10)$$

Thus, the activation energy is inversely proportional to the number of metal sites, N, over which the electron is delocalized. For two species which differ only in delocalization character, e.g., a localized species, $\Delta G^*_{loc} = \Delta G^*_1$, and an N-delocalized species, $\Delta G^*_{deloc} = \Delta G^*_N$, the relation between the barrier heights for electron transfer can be written as

$$\Delta G^*_{deloc} = f\Delta G^*_{loc} = \frac{1}{N}\Delta G^*_{loc} \quad (11)$$

Equation 11 states that the activation barrier for transfer of an N-delocalized electron is N times smaller than the barrier for transfer of a localized electron. This property is the basis for deriving the expression of the rate constant for self-exchange involving delocalized species (see below).

2.2. Activation-Energy Barrier for Electron Transfer: Nonidentical Sites. The results of the previous section can be readily generalized to the electron-transfer reaction $D_{red} + A_{ox} \rightarrow D_{ox} + A_{red}$ in which D_{red} and A_{red} are nonidentical clusters having different electron delocalization patterns ($f_D \neq f_A$). For example, Figure 1 (bottom) depicts the transfer between two trinuclear clusters with different delocalization patterns. The expression for the activation barrier can be obtained by geometrical analysis of the potential surfaces for the initial and final state of the electron-transfer process (eqs 12a,b). The

$$E_{DA}[n_D = 1] = {}^1/_2\kappa(Q_{D,s}{}^2 + Q_{A,s}{}^2) + \lambda\sqrt{f_D}Q_{D,s} + \Delta \quad (12a)$$

$$E_{DA}[n_A = 1] = {}^1/_2\kappa(Q_{D,s}{}^2 + Q_{A,s}{}^2) + \lambda\sqrt{f_A}Q_{A,s} \quad (12b)$$

potential surfaces are paraboloids of revolution centered at points I (initial state) and II (final state) of the Q-space shown in Figure 2. Parameter Δ has been introduced to adjust the relative energies of the potential minima. We assume that the reaction kinetics is determined by the barrier height for electron transfer through the saddle point, s, which is the lowest intersection point of the two paraboloids. In the case of the normal regime as defined by Marcus,[20] point s is intervening the two potential minima while in the inverted regime it is located on the line outside the segment defined by the two minima, I and II. A section of the potential wells along Q_{eff} is shown in Figure 3.

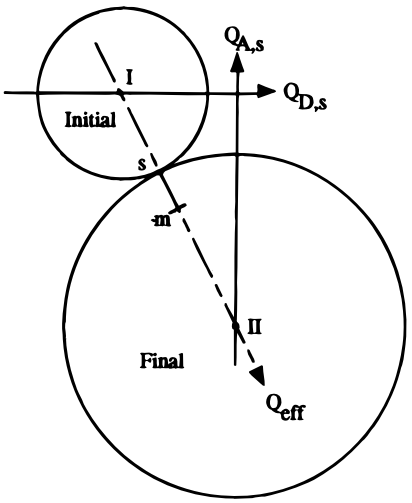

Figure 2. Space of coordinates, $Q_{D,s}$ and $Q_{A,s}$, describing the active distortions in the initial state ($D_{red}A_{ox}$) and the final state ($D_{ox}A_{red}$) of the redox reaction, respectively. The minima, at $(-\lambda\sqrt{f_D}/\kappa,0)$ and $(0,-\lambda\sqrt{f_A}/\kappa)$, of the potential wells for $D_{red}A_{ox}$ and $D_{ox}A_{red}$ are indicated by I and II, respectively. Equipotential contours for each potential are located on concentric circles centered at the corresponding minima, I and II. The f factors used are $f_D = {}^1/_2$ and $f_A = 1$ and describe a fully delocalized binuclear donor and a site-localized acceptor, respectively. Q_{eff} is the reaction coordinate of the electron-transfer reaction. s is defined as the intersection point of the two paraboloids on Q_{eff}. This location ensures its quality of saddle point. m is the point located at equal distances from I and II and coincides with s when the potential minima have equal energies. Δ has been taken equal to zero.

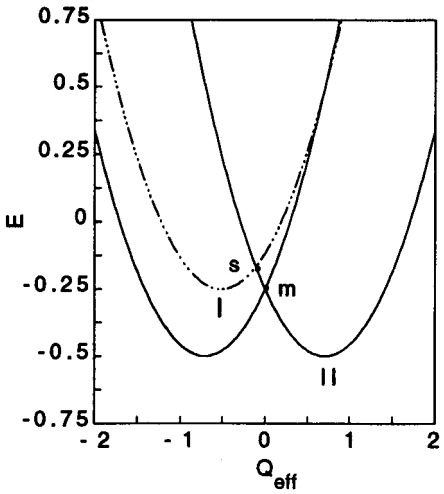

Figure 3. Section of the potential wells for the initial state $D_{red}A_{ox}$ (left) and the final state $D_{ox}A_{red}$ (right) along reaction coordinate Q_{eff} defined in Figure 2. Energies are expressed in units of χ_0. Parameters used: $f_A = 1$, $f_D = 1$ (—), $f_D = 1/2$ (— ···—), and $\Delta = 0$. Saddle point s and middle point m are indicated.

The free-energy change is given in eq 13a. The reorganization

$$\Delta G^\circ_{DA} = {}^1/_2(f_D - f_A)\chi_0 - \Delta \quad (13a)$$

$$\chi_{DA} = {}^1/_2(f_D + f_A)\chi_0 \quad (13b)$$

$$\Delta G^*_{DA} = \frac{(\chi_{DA} + \Delta G^\circ_{DA})^2}{4\chi_{DA}} \quad (13c)$$

parameter, χ_{DA} (eq 13b), is defined as the magnitude of the difference of the energies in the points I and II on one of the potential surfaces described by eq 12a or 12b. The activation energy is given in eq 13c. χ_0 is defined as λ^2/κ and represents

the reorganization parameter for electron transfer between localized species. Equations 13a and 13b have been derived by using Figures 2 and 3. For electron transfer from an *N*-delocalized donor ($f_D = 1/N$) to an *M*-delocalized acceptor ($f_A = 1/M$) the reorganization parameter is given by

$$\chi_{DA} = \chi_{N,M} = \frac{1}{2}\left(\frac{1}{N} + \frac{1}{M}\right)\chi_0 \tag{14a}$$

For $\Delta G^\circ_{DA} = 0$, the activation energy is given by

$$\Delta G^*_{N,M} = \frac{1}{4}\chi_{N,M} = \frac{1}{2}\left(\frac{1}{N} + \frac{1}{M}\right)\Delta G^*_{loc} \tag{14b}$$

Here $\Delta G^*_{loc} = \Delta G^*_{1,1} = \chi_0/4$. The expression indicates that for $\Delta G^\circ_{DA} = 0$ intramolecular electron delocalization in the donor and/or acceptor reduces the activation energy for intermolecular electron transfer. This result can be generalized to $\Delta G^\circ_{DA} < 0$: in the normal regime and for constant ΔG°_{DA}, a reaction which involves delocalized mixed-valence species has a lower activation energy than a reaction which involves localized species. In this connection, it is interesting to note that the extra electrons in the ground states of mixed-valence 3-Fe and 4-Fe clusters are delocalized over mainly two metal sites ($N \approx 2$) and that a higher degree of delocalization has been observed in an excited state of a 3-Fe cluster ($N \approx 3$).[43] Delocalization and spin state in synthetic and protein-bound $[Fe_4S_4]^+$ clusters are found to be sensitive to environment.[71−74] We note that the reorganization energy contains also outer-sphere contributions. As indicated in the Introduction, the polarization of the solvent is largely independent of intramolecular delocalization for large molecules (proteins or complexes containing bulky ligands) and may be expressed by a constant term in χ_{out}. We defer an analysis of the effect of outer-sphere reorganization energy to a future study.

2.3. Electron-Transfer Rates. For nonadiabatic electron transfer, the functional dependence of the rate constant, *k*, on the free energy of activation is given by

$$k[\Delta G^*] \propto (\Delta G^*)^{-1/2} \exp(-\Delta G^*/k_B T) \tag{15}$$

In this section we consider the case of $\Delta G^\circ = 0$ which is applicable to self-exchange. By using eqs 9 and 15, the rate constant for self-exchange can be expressed in terms of the parameters for the kinetics of the corresponding localized species (eq 16a).

$$k = k_{loc} f^{-1/2} \exp\left(\frac{(1-f)\Delta G^*_{loc}}{k_B T}\right) \tag{16a}$$

Equation 16b is the expression for the special case of an *N*-delocalized species ($f = 1/N$).

$$k_{deloc} = k_{loc} N^{1/2} \exp\left(\frac{N-1}{N}\frac{\Delta G^*_{loc}}{k_B T}\right) \tag{16b}$$

Substitution of eq 14b into eq 15 yields the expression

$$k_{deloc} = k_{loc}\left(\frac{2MN}{M+N}\right)^{1/2} \exp\left[\left(1 - \frac{M+N}{2MN}\right)\frac{\Delta G^*_{loc}}{k_B T}\right] \tag{17}$$

for the rate of transfer from an *N*-delocalized donor to an *M*-delocalized acceptor. Equation 16b follows also as special case of eq 17 by taking $N = M$. These results can be easily generalized to $\Delta G^\circ < 0$. For $\Delta G^\circ_{deloc} = \Delta G^\circ_{loc} < 0$, eq 17 gives the lower bound for the rate constant of electron transfer in the normal regime. On the basis of eqs 16 and 17, it is to be expected that *intra*molecular electron delocalization has an important impact on *inter*molecular electron-transfer kinetics (see Results and Discussion).

3. Exchange Coupling and Electron-Transfer Kinetics

The contributions to the rate constant from resonance stabilization energy in donor and acceptor cancel in self-exchange reactions. This cancellation allowed us in the previous section to consider exclusively the effect of electron delocalization on *reorganization* energy (eq 13b). However, in the case of nonidentical redox partners, the *resonance* energy is expected to affect the kinetics of the electron transfer as well. In this section, we derive an expression (eq 31) for the rate constant of electron transfer between an exchange-coupled binuclear mixed-valence donor and a diamagnetic monomeric acceptor. For these electron-transfer reactions both the reorganization energy and the resonance stabilization energy need to be considered. The latter contribution, which causes valence delocalization, will be specified. In addition, contributions to electron transfer through the excited states of the dimer will be included.

3.1. Reorganization Energy and Resonance Energy of a Mixed-Valence $[Fe_2S_2]^+$ Dimer. Let us consider an electron-transfer reaction in which an $[Fe_2S_2]^+$ cluster is the donor. Clusters of this type are found in the electron-transfer chains of many biological systems.[8] The reducing equivalent is considered to be the "extra" electron in the $[Fe^{2+}Fe^{3+}]$ unit. The iron sites of this cluster carry the spins $S_i = 2$ and $^5/_2$, respectively. The states of the mixed-valence dimer are characterized by the total spin quantum number *S* which ranges from $^1/_2$ to $^9/_2$. The extra electron is subject to *intra*molecular Fe−Fe resonance interaction (1st term in eq 18), which favors electron delocalization over the metal sites of the cluster, and to vibronic interactions (2nd term), which favor trapped electronic states. The delocalization of the extra electron acts as a ferromagnetic coupling mechanism of the iron spins; this mechanism is called double exchange. In addition, the iron spins are coupled by Heisenberg−Dirac−van Vleck (HDvV) exchange interactions (3rd term), which usually favor antiferromagnetic ordering of the metal spins. The order of the spin levels of $[Fe_2S_2]^+$ depends on the balance of the three interactions which is determined by the relative strengths of the coupling parameters in

$$\hat{H}_{D_{red}} = B\hat{T}_D + \hat{H}_{vc}(\kappa,\lambda) + (-2J\hat{S}_1\cdot\hat{S}_2 + 10J) \tag{18}$$

where *B* is the double-exchange parameter and *J* the exchange-coupling constant. For details of this theory and for the definitions of the terms in eq 18 we refer to refs 33, 35, and 66. The last term in eq 18 (and, below, in eq 26) has been chosen such that the HDvV energy of the spin state with maximum multiplicity is zero. This choice is based on Anderson's theory for exchange interaction.[67] In this theory, predominant lower-order contributions to *J* are partitioned in a ferromagnetic term, J_F ("potential" exchange), and an antiferromagnetic term, J_{AF} ("kinetic" exchange). In Fe−S clusters,

(71) Carney, M. J.; Papaefthymiou, G. C.; Whitener, M. A.; Spartalian, K.; Frankel, R. B.; Holm, R. H. *Inorg. Chem.* **1988**, *27*, 346−352.
(72) Carney, M. J.; Papaefthymiou, G. C.; Spartalian, K.; Frankel, R. B.; Holm, R. H. *J. Am. Chem. Soc.* **1988**, *110*, 6084−6095.
(73) Lindahl, P. A.; Day, E. P.; Kent, T. A.; Orme-Johnson, W. H.; Münck, E. *J. Biol. Chem.* **1985**, *260*, 11160−11173.
(74) Meyer, J.; Moulis, J.-M.; Gaillard, J.; Lutz, M. In *Iron−Sulfur Proteins*; Cammack, R., Ed.; Academic Press: San Diego, CA, 1992; Vol. 38, pp 73−115.

Table 1. Classification of Spin States of an $[Fe^{2+}Fe^{3+}]$ Dimer According to Their Delocalization Character for Different $R = |B|/\chi_0$ Ratios

condition	localized	delocalized
$R < 1/10$	$^1/_2$, $^3/_2$, $^5/_2$, $^7/_2$, $^9/_2$	
$1/10 \le R < 1/8$	$^1/_2$, $^3/_2$, $^5/_2$, $^7/_2$	$^9/_2$
$1/8 \le R < 1/6$	$^1/_2$, $^3/_2$, $^5/_2$	$^7/_2$, $^9/_2$
$1/6 \le R < 1/4$	$^1/_2$, $^3/_2$	$^5/_2$, $^7/_2$, $^9/_2$
$1/4 \le R < 1/2$	$^1/_2$	$^3/_2$, $^5/_2$, $^7/_2$, $^9/_2$
$1/2 \le R$		$^1/_2$, $^3/_2$, $^5/_2$, $^7/_2$, $^9/_2$

$|J_{AF}|$ is considerably larger than J_F, which is here taken $J_F = 0$, leading to a net antiferromagnetic coupling constant, $J < 0$. J_{AF} results from the interaction of a valence-localized ground configuration with higher-lying inter-metal charge-transfer configurations. This interaction depends essentially on the spin of the dimer; the interaction decreases with increasing spin and vanishes in the state with maximum spin multiplicity. Therefore, the HDvV energy has been taken zero in the latter state.[34,75]

Anderson and Hasegawa have shown that the resonance splitting, described by the first term of eq 18, depends on spin: $(2S + 1)|B|$.[76] The ratio between the resonance energy and the reorganization parameter, χ_0, determines the delocalization character of each spin state. If the condition given in eq 19a is

$$1 \le \frac{(2S+1)|B|}{\chi_0} \tag{19a}$$

fulfilled, the valences are (completely) delocalized (class III in the Robin and Day classification[50]). If the condition given in eq 19b is fulfilled, partial localization occurs (class II). For

$$0 < \frac{(2S+1)|B|}{\chi_0} < 1 \tag{19b}$$

$|B| = 0$, the valences are fully localized (class I). The relationship between rate constant and intramolecular electron delocalization (eq 17), in conjuction with the spin-dependent delocalization criteria (eqs 19), suggests a possible influence of spin on electron-transfer kinetics. Spin as a rate-determining factor needs to be considered, particularly when the cluster accommodates spin states with different delocalization patterns (see below). Coexistence of localized and delocalized spin states is found in the parameter range for which $^1/_{10} \le |B|/\chi_0 < ^1/_2$ (see Table 1). The f factor defined in eq 4b depends on the delocalization degree and thus on spin: $f = f_S$. The spin dependence of f can be derived from the expressions for the wave functions at the potential minima for the dimer and is given by eq 20a for a delocalized spin state (class III) and by eq 20b in the case that the electron is localized or partially localized (Class I or II).

$$f_S = {}^1/_2 \tag{20a}$$

$$f_S = 1 - \frac{1}{2}\left(\frac{(2S+1)B}{\chi_0}\right)^2 \tag{20b}$$

(75) An alternative choice in which the barycenter of the exchange-split levels is conserved has been considered in the literature.[34] However, in the context of Anderson's theory for antiferromagnetic exchange, the levels described by eqs 18 and 26 represent the lower half of a more extended space of interacting states which includes the metal−metal charge-transfer configurations. The barycenter of the energies is conserved only when the full space is considered. Therefore, the barycenters of the energies given in eqs 18 and 26 are a function of J and J', respectively.

(76) Anderson, P. W.; Hasegawa, H. *Phys. Rev.* **1955**, *100*, 675−681.

The spin-state energies are functions of B, J, and χ_0 (eqs 21a,b).[33,66] The energy of a delocalized state is given by

$$\epsilon_S^{\text{deloc}} = -{}^1/_4\chi_0 - JS(S+1) - B(S+{}^1/_2) + {}^{99}/_4\,J \tag{21a}$$

and the energy of a localized or partially localized state by

$$\epsilon_S^{\text{loc}} = -\frac{1}{2}\chi_0 - \left(J + \frac{B^2}{\chi_0}\right)S(S+1) - \frac{B^2}{4\chi_0} + {}^{99}/_4\,J \tag{21b}$$

The spin dependence of the energies for the (partially) localized states, eq 21b, is described by an effective HDvV Hamiltonian with exchange-coupling constant, $J_{\text{eff}} = J + B^2/\chi_0$, which contains a contribution for antiferromagnetic exchange (J) and a ferromagnetic contribution due to incipient double exchange (B^2/χ_0). The contributions for reorganization energy ($\epsilon_S^{\text{reorg}}$) and resonance energy plus HDvV exchange energy ($\tilde{\epsilon}_S$) to the total energy (eq 21) are specified in eq 22 and eqs 23,

$$\epsilon_S^{\text{reorg}} = -{}^1/_2\, f_S\chi_0 \tag{22}$$

$$\tilde{\epsilon}_S^{\text{deloc}} = -JS(S+1) - |B|(S+{}^1/_2) + {}^{99}/_4\,J \tag{23a}$$

$$\tilde{\epsilon}_S^{\text{loc}} = (f_S - 1)\chi_0 - JS(S+1) + {}^{99}/_4\,J \tag{23b}$$

respectively. Equation 23a applies to a fully delocalized state, and eq 23b, to a (partially) localized state. A comparison of the first term in eq 23b with eq 22 reveals that a change in the delocalization character from localized ($f_S = 1$) to partially localized ($^1/_2 < f_S < 1$) involves a gain in resonance energy equal to twice the loss in reorganization energy.[77]

3.2. Factors Affecting Activation Energy. In this section, an expression is derived for the activation energy of the reaction $D_{\text{red}} + A_{\text{ox}} \rightarrow D_{\text{ox}} + A_{\text{red}}$ in which the donor, D_{red}, is an $[Fe_2S_2]^+$ cluster in a state with spin S, and the acceptor, A_{ox}, is a diamagnetic monomeric site ($f_A = 1$). According to eq 14b, for $\Delta G^\circ_{DA} = 0$, the activation energy, $\Delta G^*_{2,1}$, is reduced by (partial) delocalization in D_{red}: $3\Delta G^*_{1,1}/4 \le \Delta G^*_{2,1} < \Delta G^*_{1,1}$. The following analysis indicates that delocalization may have a considerable impact on the reaction kinetics.

3.2.1. Spin Selection Rule. Electron-transfer interactions are essentially electrostatic in nature and, therefore, are subject to the spin selection rule, $\Delta S = 0$, the spin difference being taken between the spin quantum numbers for the initial and final state (see Scheme 1). Because upon electron transfer the acceptor site is converted from a diamagnetic state, $S_{A_{ox}} = 0$, to a paramagnetic state, $S_{A_{red}} = ^1/_2$, the spin of the oxidized donor, D_{ox}, must be $S_{D_{ox}} = S \pm ^1/_2$, in order to fulfill the triangular condition for addition of angular momenta.

3.2.2. Spin Dependence of Activation Energy. For the electron-transfer reaction given in Scheme 1, the free-energy change can be written as

$$\Delta G^\circ_{S,S\pm1/2} = \epsilon'_{S\pm1/2} - \epsilon_S - \delta \tag{24}$$

(77) In the normal regime, ΔG^* is reduced by valence delocalization (see Figure 3) and increased by resonance stabilization. The latter effect dominates the former effect, leading to a net increase in ΔG^* in the delocalized state: $\Delta G^*_{\text{loc}} < \Delta G^*_{\text{deloc}}$. As a consequence, the rate constant for transfer from a valence-localized dimer state ($B = 0$) to a given acceptor is larger than the transfer from a delocalized dimer state ($B \neq 0$) to the same acceptor, $k_{\text{loc}} > k_{\text{deloc}}$, provided that the constant energy shift, δ, defined in eq 24, has the same value in the two reactions. In addition, the net value of $-\Delta G^\circ$ is lowered by resonance interaction ($B \neq 0$). Delocalization effects on rate constant can be favorably studied in self-exchange reactions since contributions to ΔG^* from resonance stabilization in donor and acceptor cancel.

The subscripts indicate the spin of the donor in the initial state (S) and the final state ($S \pm {}^1/_2$). $\epsilon'_{S\pm1/2}$ represent the energies of the $S \pm {}^1/_2$ spin levels in D_{ox}. By analogy with the treatment given in section 3.1 for the mixed-valence cluster, these energies can be separated in contributions for reorganization energy ($\epsilon^{reorg}_{S\pm1/2}$) and HDvV exchange energy ($\tilde{\epsilon}_{S\pm1/2}$). The former contribution is given by

$$\epsilon^{reorg}_{S\pm1/2} = -{}^1/_2\chi_0 \tag{25}$$

The exchange interactions in D_{ox} are described by the HDvV Hamiltonian given in eq 26. The exchange-coupling constant

$$\hat{H}_{D_{ox}} = -2J'\hat{S}_1\cdot\hat{S}_2 + {}^{25}/_2\,J' \tag{26}$$

J' for D_{ox} may differ from the value J for D_{red}. Accordingly, the HDvV exchange contribution to the energies of the spin levels in D_{ox} are

$$\tilde{\epsilon}'_{S\pm1/2} = -J'(S \pm {}^1/_2)(S \pm {}^1/_2 + 1) + 30J' \tag{27}$$

Parameter δ (eq 24) is a spin-independent energy shift which is defined as the difference of the energies of the initial and the final state as obtained for $B = J = J' = \chi_0 = 0$.

The free-energy change of the reaction can be rewritten as

$$\Delta G^\circ_{S,S\pm1/2} = {}^1/_2(f_S - 1)\chi_0 + \tilde{\epsilon}'_{S\pm1/2} - \tilde{\epsilon}_S - \delta \tag{28a}$$

A comparison of eq 28a with eq 13a shows that the sum of the last three terms can be identified with $-\Delta$. According to eq 13b, the reorganization parameter can be expressed as

$$\chi_S = {}^1/_2(f_S + 1)\chi_0 \tag{28b}$$

The activation energy for electron transfer from the state S of D_{red} is given in eq 28c.

$$\Delta G^*_{S,S\pm1/2} = \frac{(\chi_S + \Delta G^\circ_{S,S\pm1/2})^2}{4\chi_S} \tag{28c}$$

By combination of eqs 28a−c, an expression for the activation barrier is obtained:

$$\Delta G^*_{S,S\pm1/2} = \frac{(f_S\chi_0 + \tilde{\epsilon}'_{S\pm1/2} - \tilde{\epsilon}_S - \delta)^2}{2(f_S + 1)\chi_0} \tag{29}$$

The choice of expressions for f_S (eq 20a or 20b) and $\tilde{\epsilon}_S$ (eq 23a or 23b) is prescribed by the delocalization condition given in eqs 19 (i.e., eqs 20a, 23a for delocalized states and eqs 20b, 23b otherwise).

3.2.3. Spin-Projection Factors. The transfer-matrix elements depend also on spin-projection factors which account for the change in spin coupling in the transition from the initial state to the final state. Thus, the extra electron with spin s, which is initially coupled to the spin, s', of the electron with which it shares the ground orbital in d^6 configurations, is coupled in the final state to resultant spin, $S \pm {}^1/_2$, of D_{ox}. By using Racah's technique for recoupling of angular momenta,[78] we obtained the expressions for the spin factors in the square of the electronic matrix elements, $(H_{DA}^{S,S\pm1/2})^2 = P_{S,S\pm1/2}H_{DA}^2$, that are given in eq 30.

Scheme 1

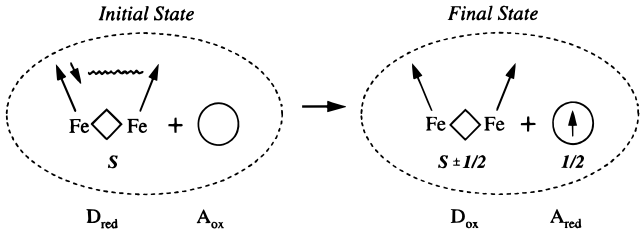

$$P_{S,S\pm1/2} = {}^1/_{10}[6 \pm (S + {}^1/_2)] \tag{30}$$

3.2.4. Site-Dependent Factor. Let us assume that the orbital, $|\varphi_{D,1}\rangle$, containing the extra electron at metal site 1 of the binuclear donor cluster is connected to the acceptor orbital, $|\varphi_A\rangle$, by a nonzero matrix element for electron transfer, $\langle\varphi_{D,1}|\hat{T}_{DA}|\varphi_A\rangle = H_{DA} \neq 0$, and that the transfer interaction from site 2 vanishes, $\langle\varphi_{D,2}|\hat{T}_{DA}|\varphi_A\rangle = 0$.[79] The fractional probability of the extra electron to occupy the transfer site 1 of the donor is given by the square of the mixing coefficient, $c_{D,1}^2$. Thus, the rate constant, which depends on the square of the transfer-matrix element (see Introduction), is proportional to $c_{D,1}^2$. This implies that in fully delocalized states, $|\psi_D\rangle = (|\varphi_{D,1}\rangle \pm |\varphi_{D,2}\rangle)/\sqrt{2}$, the electron-transfer rate depends on the factor $H_{DA}^2/2$.[80] In the case of (partial) localization, the electronic states are associated with the two minima of a double-well potential. If the wave function at one of the minima is written as $|\psi_D\rangle = c_{D,1}|\varphi_{D,1}\rangle + c_{D,2}|\varphi_{D,2}\rangle$, then the wave function at the other minimum is obtained by interchanging the mixing coefficients, $|\psi'_D\rangle = c_{D,2}|\varphi_{D,1}\rangle + c_{D,1}|\varphi_{D,2}\rangle$. Addition of the contributions for the transfer from site 1 in the two minima yields the factor $H_{DA}^2(c_{D,1}^2 + c_{D,2}^2) = H_{DA}^2$, where we have used the normalization condition for the wavefunctions.

3.3. Electron-Transfer Rate Constant. The factors described in the previous sections can be combined with the expression given in the Introduction to yield the rate constant for nonadiabatic electron transfer from a state with spin S of the dimer $[Fe_2S_2]^+$ to a diamagnetic monomer in semiclassical approximation (eq 31a). For this spin level, the contributions

$$k_S = (2\pi)^{1/2}\hbar^{-1}H_{DA}^2(\chi_0 k_B T)^{-1/2}\sum_{\sigma=-1/2}^{+1/2} r_S P_{S,S+\sigma}(1 + f_S)^{-1/2} \exp(-\Delta G^*_{S,S+\sigma}/k_B T) \tag{31a}$$

for the two final states, $S \pm {}^1/_2$, are summed. The summation contains the following preexponential factors: r_S is a reduction factor of H_{DA}^2 due to delocalization ($r_S = {}^1/_2$ if the delocalization condition, eq 19a, is fulfilled, and $r_S = 1$ otherwise), $P_{S,S\pm1/2}$ is the spin factor given in eq 30, and the next factor originates from the delocalization-related change in the reorganization parameter, χ_{DA}. The numerator in the argument of the exponential function is the activation energy given in eq 29. Using eq 31a, the total rate constant for electron transfer from the exchange-coupled $[Fe_2S_2]^+$ cluster to a diamagnetic monomer can be written as the Boltzmann-weighted summation of

(78) Tinkham, M. *Group Theory and Quantum Mechanics*; New York: McGraw-Hill, 1964.

(79) This assumption is arbitrary but has little impact on the general trend in the results. When the transfer from the second site is set equal to that from the first site, the value for the rate constant is doubled.

(80) Under the assumption of strong double exchange, the upper state of any pair of delocalized states with equal spin is high in energy; therefore, its contribution to the electron-transfer process can be ignored.

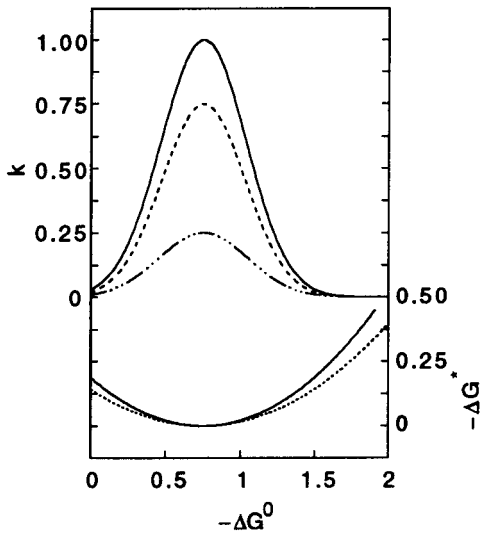

Figure 4. Top panel: Rate constant normalized to its maximum, k/k_{max} (—); ground state, k_{gr}/k_{max} (- - -); and excited state, k_{ex}/k_{max} (— ··· —), relative contributions to the rate constant (defined in text). Bottom panel: activation energies, $\Delta G^*_{S,S+1/2}$, obtained for $S = {}^1/_2$ (···) and $S = {}^9/_2$ (—) as a function of $-\Delta G°$. Energies are expressed in units of χ_0. Parameter values used: $J = J' = 0$ cm^{-1}; $\chi_0 = 4000$ cm^{-1}; $B = 400$ cm^{-1}; T = 300 K. The increasing energy order and delocalization patterns are as follows: $({}^9/_2)_{loc-deloc}$, $({}^7/_2, {}^5/_2, {}^3/_2, {}^1/_2)_{loc}$. The $S = {}^9/_2$ ground state is separated by 150 cm^{-1} from the first excited state, $S = {}^7/_2$.

contributions to electron transfer from ground and excited states in the spin ladder of D_{red}:

$$k = \frac{1}{Z}\sum_{S=1/2}^{9/2}(2S+1)k_S \exp(-\epsilon_S/k_BT) \qquad (31b)$$

$$Z = \sum_{S=1/2}^{9/2}(2S+1)(2r_S)\exp(-\epsilon_S/k_BT) \qquad (31c)$$

where Z is the partition function, $2S + 1$ is the spin multiplicity, and $2r_S$ accounts for the 2-fold degeneracy of the (partially) localized states of D_{red}. The energy of spin state S of D_{red}, ϵ_S, is given by eqs 21.

4. Results and Discussion

4.1. Analysis of the Influence of Double Exchange and HDvV Exchange on Electron Transfer from $[Fe_2S_2]^+$. In this section, we present the results for the rate constant of the electron-transfer reaction $D_{red} + A_{ox} \rightarrow D_{ox} + A_{red}$, where D_{red} is the mixed-valence cluster $[Fe_2S_2]^+$ and A_{ox} is a diamagnetic mononuclear electron acceptor. By using eq 31, the rate constants presented in Figures 4 and 5 have been calculated as a function of the difference, $-\Delta G°$, between the ground-state free energies for the initial and the final state:

$$-\Delta G° = {}^1/_2(1 - f_{S_{gr}})\chi_0 - 30J' + \tilde{\epsilon}_{S_{gr}} + \delta \qquad (32)$$

where S_{gr} is the spin of the ground state of D_{red}. The value of $-\Delta G°$ differs from δ due to contributions for vibronic coupling, HDvV exchange, and double exchange. The $\Delta G°$ values considered in the plots cover the upper part of the exoergic reaction range: $-2\chi_0 \le \Delta G° \le 0$. Because this study focuses on the donor site, the redox potential for the couple $A_{ox} \leftrightarrow A_{red}$ will be considered as a fixed quantity. With this assumption, variations in $-\Delta G°$ derive uniquely from changes in the redox potential for the couple $D_{red} \leftrightarrow D_{ox}$. In particular, the redox potential for the donor becomes more reductive in going from the left to the right along the abscissas in Figures 4 and 5. The graphs for the activation energies, $\Delta G^*_{S,S+1/2}$, $S = {}^1/_2, ..., {}^9/_2$, are also given in these figures.[81] The minimum in each $\Delta G^*_{S,S+1/2}$ curve separates the normal electron-transfer regime (left from minimum) from the inverted electron-transfer regime (right from minimum)[20] and defines the position of the maximum of the corresponding k_S graph (not shown). The bell-shaped curves for k shown in Figures 4 and 5 are obtained by taking the Boltzmann-weighted sum of the graphs for k_S, according to eq 31b. The maximum of k is located in the vicinity of the activation-energy minimum for the ground state. The width of the k graphs depends on temperature and narrows significantly by cooling the system. However, because the systems of our interest operate under physiological conditions, the temperature has been taken as 300 K throughout the calculations. The contributions of the ground and excited states to the rate constant, denoted as k_{gr} and k_{ex}, respectively, are also presented in the figures.[82]

In Figure 4, we present the results for weak double exchange (i.e., $|B|/\chi_0 \le {}^1/_{10}$) and vanishing HDvV exchange ($J = J' = 0$). For the parameters adopted (see figure caption), the ground state spin of D_{red} is ${}^9/_2$ and the states are partially localized or on the edge of delocalization. The levels appear in the ascending energy order $({}^9/_2)_{loc-deloc}$, $({}^7/_2, {}^5/_2, ..., {}^1/_2)_{loc}$. The minima of the $\Delta G^*_{S,S+1/2}$ graphs in Figure 4 coincide at the spin-independent value given in eq 33. As a consequence, the

$$(-\Delta G°_{min})^{loc} = \chi_0 - \frac{25B^2}{\chi_0} \qquad (33)$$

positions of the maxima in k_{gr} and k_{ex} coincide as well (see Figure 4). Hence, the kinetics in the localized, weak double-exchange case is rather insensitive to the actual thermal distribution over the spin levels: the ground- and excited-state contributions are indistinguishable.

In Figure 5, we consider the case of strong double exchange ($|B|/\chi_0 \ge {}^1/_{10}$) in the presence of antiferromagnetic HDvV exchange ($J = J' < 0$). Using the parameters of Figure 5, the spin levels of D_{red} appear in the same energy order as those for Figure 4 but the delocalization patterns have changed to $({}^9/_2, {}^7/_2, {}^5/_2)_{deloc}$, $({}^3/_2)_{loc-deloc}$, $({}^1/_2)_{loc}$. The bell-shaped k curve in Figure 5 is less symmetric than the corresponding curve in Figure 4. This change is caused by a combination of two factors: (1) dispersion along the abscissa of the minima in $\Delta G^*_{S,S+1/2}$ for the different spin states (see figure) and (2) significant thermal population of the excited states. For $S_{gr} = {}^9/_2$, eqs 34 give the positions of the minima of $\Delta G^*_{S,S+1/2}$.[83]

$$(-\Delta G°_{min})^{loc} = {}^5/_4\chi_0 - 30J - 5|B| + ({}^9/_2 - S_{loc})J \qquad (34a)$$

$$(-\Delta G°_{min})^{deloc} = {}^3/_4\chi_0 - 30J + ({}^9/_2 - S_{deloc})(J - |B|) \qquad (34b)$$

These values are functions of the spin. HDvV exchange gives rise to identical spin-dependent terms in eq 34a and eq 34b, while double exchange contributes a spin-dependent term only in the delocalized case. The dispersion of the minima, which for the parameter values of Figure 5 is mainly determined by

(81) $\Delta G^*_{S,S+1/2} = \Delta G^*_{S,S-1/2}$ for $J' = 0$, while the two barriers differ for $J' \neq 0$. Since the spin-dependent factors given in eq 30 have larger values for the + sign than for the − sign, only the barriers obtained for the + sign are presented.

(82) k_{gr} and k_{ex} are evaluated by confining the summation in eq 31b to, respectively, the ground and the excited spin states for D_{red}.

(83) The expressions for $(-\Delta G°_{min})^{loc}$ given in eqs 33 and 34a differ even for $J = J' = 0$ due to the different character (viz. localized and delocalized, respectively) of the corresponding $S = {}^9/_2$ ground states.

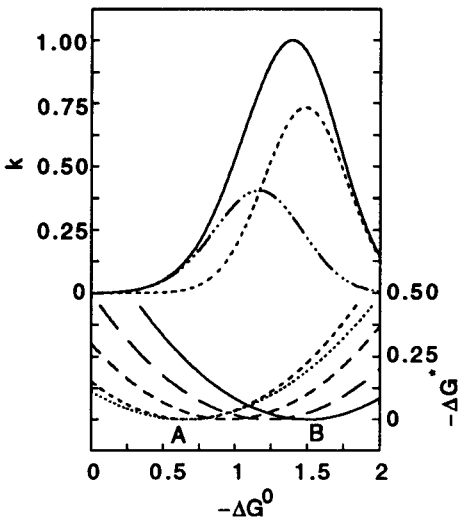

Figure 5. Top panel: Rate constant normalized to its maximum, k/k_{max} (—); ground state, k_{gr}/k_{max} (- - -), and excited state, k_{ex}/k_{max} (— ··· —), relative contributions to the rate constant (defined in text). Bottom pannel: activation energies, $\Delta G^*_{S,S+1/2}$, obtained for $S = {}^1/_2$, ${}^3/_2$, ${}^5/_2$, ${}^7/_2$, ${}^9/_2$, as a function of $-\Delta G°$. Energies are expressed in units of χ_0. The plot of activation energy for $S = {}^9/_2$ is indicated by a solid line; the activation energies for the other spin states are indicated by broken lines of which the hash lengths decrease in the order ${}^7/_2$, ${}^5/_2$, ${}^3/_2$, ${}^1/_2$. Points A and B correspond to the minima in the $\Delta G^*_{1/2,1}$ and $\Delta G^*_{9/2,5}$ curves, respectively. Parameter values used: $J = J' = -100$ cm^{-1}; $\chi_0 = 4000$ cm^{-1}; $B = 1000$ cm^{-1}; T = 300 K. The increasing energy order and delocalization patterns are as follows: $({}^9/_2,{}^7/_2,{}^5/_2)_{deloc}$, $({}^3/_2)_{loc-deloc}$, $({}^1/_2)_{loc}$. The $S = {}^9/_2$ ground state is separated by 100 cm^{-1} from the first excited state, $S = {}^7/_2$.

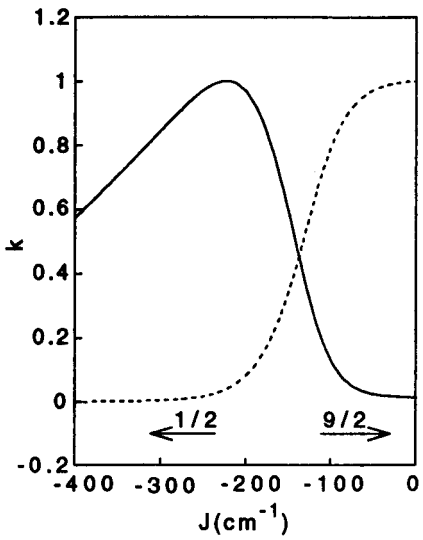

Figure 6. Rate constant normalized at its maximum, k/k_{max}, as a function of the exchange-coupling constant J, obtained for $\delta = 3600$ cm^{-1} (—) and $\delta = 7000$ cm^{-1} (- - -). Values for the exchange-coupling constants in D_{red} and D_{ox} are taken as equal, $J = J'$. J ranges for which the ground-state spin is $S = {}^1/_2$ and $S = {}^9/_2$ are indicated by arrows. Other parameter values used: $B = 1000$ cm^{-1}; $T = 300$ K.

double exchange ($|B| \gg |J|$), leads to relative displacements of the maxima in the graphs for k_S (not shown) and asymmetric broadening of the bell-shaped k curves. The displacements are reflected by the separation of the maxima of k_{gr} and k_{ex} in Figure 5. It can be seen from the figure that k_{ex} is larger than k_{gr} in a large interval of $-\Delta G°$ values; at the low end of this range, the electron transfer takes place almost entirely through excited states. The prevalence of the excited states is determined by Boltzmann factors and the relative magnitude of the activation barriers for the ground and excited states. In Figure 5, it can be seen that the interval where the $S_{gr} = {}^9/_2$ ground state has the highest activation energy (lower panel) coincides with the range in which k_{ex} is larger than k_{gr} (upper panel). For $S_{gr} = {}^9/_2$, eqs 34 also indicate that when J changes by ΔJ, the position of the maximum in k is displaced by a spin-independent value $-30\Delta J$ (compare Figures 4 and 5).

As a consequence of the spin-selection rules, the orderings of the dimer spin levels in the initial and final state of the electron-transfer process are important rate-determining factors. The initial and final state for the reaction considered in Figure 5 accommodate inverted energy level schemes, i.e. $({}^9/_2) < ... < ({}^1/_2)$ and $(0) < ... < (5)$, respectively. Thus, the ground level of the initial state, $S_{gr} = {}^9/_2$, is connected to the two highest spin levels, $S = 4$ and 5, of the final state, while the highest level of the initial state, $S_{ex} = {}^1/_2$, is connected to the two lowest levels of the final state, $S = 0$ and 1. At $\Delta G° \approx 0$, the activation energy for transfer from the $S_{gr} = {}^9/_2$ state is larger than the activation energy for transfer from states of lower spin. Hence, the rate constant for transfer from the ground state is smaller than for transfers from the excited states, i.e., $k_{9/2} < k_{S<9/2}$. Beside $\Delta G^*_{S,S+1/2}$, the energy range spanned by the spin states of D_{red} is also an important factor for electron transfer. Double exchange in D_{red} narrows the energy interval obtained from HDvV exchange and makes it smaller than in D_{ox}. This circumstance makes excited levels of the initial state thermally accessible at room temperature. The combination of the thermal accessibility and the higher rate constants for the excited levels explains the predominance of the electron transfer via excited states near the origin in Figure 5. The small spread of the initial-state spin levels readies the system for reversal of the energy order to $({}^1/_2) < ... < ({}^9/_2)$ induced by a moderate increase in the antiferromagnetic coupling, J (see section 4.2). By contrast, moderate changes in J do not change the overall arrangement of the graphs for the activation barriers shown in Figure 5, lower panel. The latter feature is expressed by eqs 34 according to which the positions of the minima are insensitive to the $-JS$ terms, provided that $|J| \ll |B|$. The insensitivity is illustrated by the near coincidence of the barrier minima for the localized states at point A in Figure 5. Thus, an increase in $-J$ can revert the energy order of the spin states while retaining their electron-transfer characteristics, i.e., the ground-state spin changes from ${}^9/_2$ to ${}^1/_2$ while the order $k_{1/2} \gg k_{9/2}$ is unchanged. A reordering of the level energies has a dramatic effect on the thermal population of a given spin state. In the example of Figure 5, stabilization of $S_{gr} = {}^1/_2$ by increasing the value of $-J$ would determine a shift of the maximum of k from the position of the zero barrier for $S_{gr} = {}^9/_2$ (minimum in right curve of lower panel) to the position of the zero barrier for $S_{gr} = {}^1/_2$ (minimum in left curve).

The preceding discussion suggests that exchange interactions have a considerable impact on the electron-transfer properties of the cluster. In Figure 6, we show the dependence of the rate constant on exchange coupling as obtained by eq 31 for two values of δ. These δ values, 3600 and 7000 cm^{-1}, correspond to the $-\Delta G°$ positions (eq 32) of the minima in the $\Delta G^*_{1/2,1}$ and $\Delta G^*_{9/2,5}$ curves, respectively, indicated by A and B in Figure 5. In contrast to the $-\Delta G°$ positions of the minima for $\Delta G^*_{S,S+1/2}$, which depend significantly on J (see eq 34), the δ values defining the minima are independent of J for $S = {}^9/_2$ and are nearly independent of J for $S < {}^9/_2$ if $|J| \ll |B|$. Therefore, the curves in Figure 6 present the k values calculated at the minima of $\Delta G^*_{1/2,1}$ and $\Delta G^*_{9/2,5}$. For example, for $J = -100$ cm^{-1} the ground state has $S_{gr} = {}^9/_2$ and, as a consequence, the maximum in the k curve is located near the minimum of $\Delta G^*_{9/2,5}$ (point B in Figure 5). As it can be seen in Figure 5, the rate constant corresponding to $\delta = 7000$ cm^{-1} is larger than

the rate constant obtained for $\delta = 3600\ cm^{-1}$. Accordingly, in Figure 6, the value on the $\delta = 7000\ cm^{-1}$ curve is larger than the value on the $\delta = 3600\ cm^{-1}$ curve at $J = -100\ cm^{-1}$. By increasing $|J|$, the spin of the ground state of D_{red} changes, via a range of intermediate spin, $^3/_2 \le S_{gr} \le {}^7/_2$, to $S_{gr} = {}^1/_2$ (left arrow).[84] The maximum of the k curve is now located in the vicinity of the minimum of the $\Delta G^*_{1/2,1}$ curve (point A in Figure 5). Hence, in Figure 6, for large values of $-J$, the curve for $\delta = 7000\ cm^{-1}$ runs below the $\delta = 3600\ cm^{-1}$ curve.

4.2. Biological Relevance of HDvV Exchange and Double Exchange. The results of the previous section reveal that the rate constant for electron transfer from mixed-valence metal clusters depends sensitively on the interplay of HDvV exchange and double exchange. In this section, we discuss the possible relevance of these theoretical results for biological electron transfer.

The steep change in the rate constant as a function of the exchange-coupling constant, J (see Figure 6), suggests that a metal cluster can act as a molecular switch for exchange-controlled electron gating. The great sensitivity of the rate constant to exchange coupling may turn this interaction into a factor relevant for the specificity of biological electron-transfer reactions. Thus, in the absence of the substrate, the cluster would be located in the slow-transfer regime (for $\delta = 7000\ cm^{-1}$, Figure 6, left). Exchange-coupling constants are known to depend sensitively on changes in molecular geometry.[85,86] Therefore, J could change by a substrate-induced conformational change and the cluster would be activated for electron transfer as a result of a shift into the fast-transfer regime (Figure 6, right). These considerations may also apply to the interpretation of the role of "effector" proteins, also described as "gating" proteins.[87,88] The sense of the variation in k as a function of J depends on δ (see Figure 6). Hence, the latter parameter could direct the electron transfer from a cluster which is the "node" of bifurcating electron-transfer pathways.

The theoretical analysis in the previous section has indicated that electron transfer through the excited states of an exchange-coupled cluster can be considerably faster than the transfer from the ground state. In particular, the excited states were found to sustain electron transfer toward environments with negative potentials (Figure 5, left). These conditions may occur in the electron-transfer reactions from the P cluster to the Fe−Mo cofactor in the MoFe protein of nitrogenase, especially in the higher reduction steps, E_3 or E_4 (Thorneley−Lowe scheme), in which the cofactor is converted into a competent intermediate for nitrogen fixation.[89,90] Contributions from the excited states of the P cluster may facilitate these critical electron-transfer steps.

Although a direct experimental proof for the coexistence of localized and delocalized states in the spin ladder of $[Fe_2S_2]^+$ clusters is still lacking, such a possibility is definitely supported by studies of diiron mixed-valence compounds. Recently, MCD, Mössbauer and EPR studies were conducted on the Cys56Ser mutant 2-Fe ferredoxin from *C. pasteurianum*, a protein in which one of the terminal cysteinyl ligands of the $[Fe_2S_2]$ core is replaced by serine by site-directed mutagenesis.[52,53] These analyses revealed the presence of a delocalized $S = {}^9/_2$ ground state in a fraction of the protein molecules. The delocalization is remarkable because it occurs despite the purported inequivalency of the iron sites created by the serine coordination at one of them. Delocalization in the presence of trapping forces attests to strong double exchange. Because the cysteinyl coordination of the $[Fe_2S_2]^+$ cores in wild-type 2-Fe ferredoxins is more symmetric than the mixed cysteinyl−serine (or solvent) coordination of the cluster in the mutant, it is to be expected that the $S = {}^9/_2$ excited state of the 2-Fe clusters in the wild-type proteins is delocalized as well. This expectation and the localized character of the $S = {}^1/_2$ ground state found in all common $[Fe_2S_2]^+$ clusters support the notion that localized and delocalized states coexist. Strong double exchange ($B \approx 1000\ cm^{-1}$) has been inferred also for plant-type ferredoxins.[55,56] As can be seen in Table 1, for the latter value of B, the states $S = ({}^1/_2)_{loc}$ and $S = ({}^9/_2)_{deloc}$ retain their delocalization character for $2000\ cm^{-1} \le \chi_0 \le 10\,000\ cm^{-1}$. The stabilization of an $S = ({}^1/_2)_{loc}$ ground state requires strong antiferromagnetic exchange coupling, while an $S = ({}^9/_2)_{deloc}$ ground state occurs for weak HDvV coupling. The change in J necessary for converting the ground state from $S = ({}^1/_2)_{loc}$ to $S = ({}^9/_2)_{deloc}$ depends on χ_0. The conversion takes place through a J range in which the ground state has intermediate spin. In the limit $\chi_0 = 10\,000\ cm^{-1}$, the J range with intermediate spin contracts to a single point.[53,66] Therefore, a small change in J can determine a reordering of the spin levels and can tune the electron-transfer rate.

The samples of the Cys56Ser mutant described in refs 52 and 53 contained variable amounts of the $S = ({}^1/_2)_{loc}$ and $S = ({}^9/_2)_{deloc}$ species depending on preparation conditions. In particular, it was shown that a considerable fraction of the clusters with an $S = ({}^1/_2)_{loc}$ ground state in the initial solution were converted to clusters with an $S = ({}^9/_2)_{deloc}$ ground state by adding glycerol to the samples. While it is unlikely that glycerol can affect the chemical structure of the cluster, geometrical distortions may be imposed on it via glycerol-induced changes in protein conformation. Subtle changes in the cluster environment can change the J value and alter the order of the spin levels.

4.3. Effect of Coupling to Symmetric Distortions on Reorganization Energy. In this section, we discuss another aspect of the effect of electron delocalization on the reorganization energy pertaining to electron transfer. This qualitative analysis bears on a recent study of the intervalence transition in the valence-delocalized dimer $[Fe_2(OH)_3(tmtacn)_2]^{2+}$.[55,56] Let us consider the reduction of a binuclear compound from the $[Fe^{3+}Fe^{3+}]$ state to a valence-delocalized $[Fe^{2.5+}Fe^{2.5+}]$ state. As it was argued above, the activation barrier for such a process depends on a symmetric distortion[91] that is an in-phase combination of breathing modes for the individual metal sites. The metal−ligand distances in the dimer increase in response to the *antibonding* metal−ligand interactions introduced by the extra electron upon reduction, leading to an overall expansion of the central core of the dimer and an *increase* of the Fe−Fe distance. In addition to the *antibonding* metal−ligand interactions, a *bonding* resonance metal−metal interaction, described by the double-exchange parameter, B, is active. The bonding character of the metal−metal interaction in $[Fe_2(OH)_3(tmtacn)_2]^{2+}$ is reflected by the dependence of B on the intermetal distance, $d|B|/dR_{Fe-Fe} < 0$.[55,56] In order to maximize this interaction, the Fe−Fe distance *decreases*. As a consequence, the contributions for the two electronic interactions to the vibronic coupling

(84) Figure 2, ref 53.
(85) Kahn, O. *Molecular Magnetism*; New York: VHC Publishers, Inc., 1993.
(86) Willett, R. D.; Gatteschi, D.; Kahn, O. *Magneto-Structural Correlations in Exchange-Coupled Systems*; Reidel: Dordrecht, The Netherlands, 1985.
(87) Wallar, B. J.; Lipscomb, J. *Chem. Rev.* **1996**, *96*, 2625−2658.
(88) Pikus, J. D.; Studts, J. M.; Achim, C.; Kauffmann, K. E.; Münck, E.; Steffan, R. J.; McClay, K.; Fox, B. G. *Biochemistry* **1996**, *35*, 9106−9119.
(89) Burgess, B. K.; Lowe, D. J. *Chem. Rev.* **1996**, *96*, 2983−3011.
(90) Howard, J. B.; Rees, D. C. *Chem. Rev.* **1996**, *96*, 2965−2982.
(91) Reimers, J. R.; Hush, N. S. *Chem. Phys.* **1996**, *208*, 177−193.

constant of the symmetric mode (partially) cancel, leading to a smaller value for the reorganization energy than expected on the basis of the metal−ligand interactions only.

4.4. Application of the Model to Self-Exchange of Binuclear Mn Compounds. In this section, we analyze the influence of intramolecular electron delocalization via changes in χ_{in} on the kinetics of self-exchange reactions in the series of manganese compounds mentioned in the Introduction.[58] Specific considerations apply to this type of reactions. Thus, beside the factors occurring in the expression for nonadiabatic electron transfer given in the Introduction, the rate constant depends on a factor representing steric effects (S_{as}) and an association constant (K).[20] The parameters H_{DA}, S_{as}, and K occur in the preexponential factor; hence, their effect on the rate constant is probably less important than that of the parameters contained in the exponential. It is likely that variations in H_{DA}, S_{as}, K, and χ_{out} are minor for self-exchange in series of homologous compounds.[92] Moreover, because $\Delta G^\circ = 0$ for these reactions, substitution of $\chi = \chi_{in} + \chi_{out}$ in the exponential factor allows separation into factors depending on χ_{in} and χ_{out}. On the basis of these arguments, we assume that the preexponential factor and the exponential factor depending on χ_{out} are constants. With these assumptions, the ratios of rate constants for self-exchange of homologous compounds depend only on χ_{in}.

The Mn compounds considered here contain the motif $[N_4MnO_2MnN_4]^{3+/2+}$, where the core oxidation levels represent the formal $Mn^{3+}-Mn^{4+}$ and $Mn^{3+}-Mn^{3+}$ states, respectively.[93−102] In the mixed-valence state, the spins of the Mn^{3+} ($t_{2g}^3e_g^1$, $S = 2$) site and the Mn^{4+} (t_{2g}^3, $S = {}^3/_2$) site are antiferromagnetically coupled to give an $S = {}^1/_2$ ground state; the reduced state comprises two Mn^{3+} sites antiferromagnetically coupled to give a diamagnetic ground state. Comparative studies of the structure data indicate that three of the compounds,[98] i.e., $[Mn_2(tmpa)_2O_2]^{3+/2+}$, $[Mn_2(bpy)_4O_2]^{3+/2+}$, and $[Mn_2(phen)_4O_2]^{3+/2+}$ are firmly valence-localized (class I), whereas a fourth compound, $[Mn_2(bispicen)_2O_2]^{3+/2+}$, is almost delocalized (class II/III). The self-exchange reactions imply the transfer of a hole from the mixed-valence state to the reduced state. The rate constant for the partially-delocalized compound is 260 to ∼1000 times larger than those of the localized compounds.[58]

Our model is used here as a first step in the analysis of the experimentally observed correlation between structural and kinetic data; a more rigorous treatment would have to be extended to account for the fact that the acceptor is also an exchange-coupled dimer. Because the exchange-coupling constant in dioxo-bridged $Mn^{3+/4+}$ dimers is large, $J < -100$ cm^{-1},[94−97,103,104] excited states are expected to be high in energy. The minima of the activation barriers almost coincide because the compounds belong to class I or II (see Figure 4). Therefore, the excited-state contributions for these compounds, with the possible exception of the bispicen complex, are small and indistinguishable from the ground-state contribution, allowing us to consider only the latter contribution. The differences between the corresponding metal−ligand bond lengths at the two metal sites in the mixed-valence dimers have been used by Monzyk and Holwerda to estimate the degree of delocalization. We use the same experimental parameters to evaluate the f factors for these compounds. In the completely localized class I case, the coordination sphere of the hole-containing site, Mn^{4+}, is distorted by $q_{loc}^{(0)} = \lambda/\kappa$, while the environment of Mn^{3+} remains unaltered, $q_2^{(0)} = 0$. Thus, in class I compounds, the bond-length difference, $\Delta(M-L)_{loc}$, is equal to λ/κ. In the partially-delocalized class II case, the relative bond-length differences can be written as

$$\frac{\Delta(M-L)}{\Delta(M-L)_{loc}} = \frac{q_1^{(0)} - q_2^{(0)}}{q_{loc}^{(0)}} = \frac{q_1^{(0)} - q_2^{(0)}}{\lambda/\kappa} = c_1^2 - c_2^2 \quad (35)$$

By using eq 35 and the normalization condition, $c_1^2 + c_2^2 = 1$, the factor $f = c_1^4 + c_2^4$ can be expressed in bond-length differences:

$$f = \frac{1}{2}\left[1 + \left(\frac{\Delta(M-L)}{\Delta(M-L)_{loc}}\right)^2\right] \quad (36)$$

We adopt $[Mn_2(tmpa)_2O_2]^{2+/3+}$ as a representative example for the localized compounds. Because the tmpa compound is fully localized,[95] its f factor is set equal to 1 (eq 36). The calculation of the reorganization energies associated with the bond-length differences requires knowledge of the force constants for the corresponding bond stretches. As these values are lacking, we have adopted the average force constant, $\kappa_L = \kappa = 2$ mdyne/Å used in ref 98. The reorganization energy depends on three bond-length differences, which for the bispicen complex are $\Delta(Mn-N_{ax}) = 0.077$ Å, $\Delta(Mn-N_{eq}) = 0.000$ Å, and $\Delta(Mn-O) = 0.040$ Å. The corresponding values, $\Delta(M-L)_{loc}$, for the tmpa complex are 0.220, 0.026, and 0.061 Å. Substitution of these values in eq 36 yields different f factors, i.e., 0.56, 0.50, and 0.71, respectively. The spread in these values points to the limitations of the model. Under the assumption of equal κ_L values for the bond stretches, the major contribution to the reorganization energy is associated with the largest bond-length difference, i.e., with $\Delta(Mn-N_{ax})$. For this reason, we consider this bond length as the most relevant indicator of delocalization degree and we use the corresponding f value, i.e. 0.56, in the interpretation of the kinetic data. The reorganization parameter that we used, i.e. $\chi_0 = 10633$ cm^{-1}, has been obtained by summing the contributions for the individual M−L bonds for the tmpa complex: $\chi_0 = \sum_L \lambda_L^2/\kappa_L = \sum_L \kappa_L (q_{L,loc}^{(0)})^2$.[98] This large value for χ_0 is supported by electronic spectroscopy data. Thus, in the case of class II dimers, the energy of the intervalence band found at 800 nm (12 500 cm^1) in the spectra of the phen-,[101] bpy-,[94,101] cyclam-,[96] and bispicen-based[97]

(92) The preexponential factor reflects also the electrostatic repulsion between the 3+ charged hole donor and the 2+ charged acceptor. This interaction is affected by electron delocalization in the mixed-valence partner of the reaction. The large size of the molecules containing the cluster mitigates this effect of delocalization by a mechanism analogous to that described for the solvation energy in the Introduction. This supports the assumption that the preexponential factor is constant.

(93) Plaksin, P. M.; Stoufer, R. C.; Mathew, M.; Palenik, G. J. *J. Am. Chem. Soc.* **1972**, *94*, 2121−2122.
(94) Cooper, S. R.; Dismukes, G. C.; Klein, M. P.; Calvin, M. *J. Am. Chem. Soc.* **1978**, *100*, 7248−7252.
(95) Suzuki, M.; Tokura, S.; Suhara, M.; Uehara, A. *Chem. Lett. (Jpn.)* **1988**, 477−480.
(96) Goodson, P. A.; Hodgson, D. J.; Michelsen, K. *Inorg. Chim. Acta* **1990**, *172*, 49−57.
(97) Goodson, P. A.; Glerup, J.; Hodgson, D. J.; Michelsen, K.; Pedersen, E. *Inorg. Chem.* **1990**, *29*, 503−508.
(98) Stebler, M.; Ludi, A.; Bürgi, H. B. *Inorg. Chem.* **1986**, *25*, 4743−4750.
(99) Towle, D. K.; Botsford, C. A.; Hodgson, D. J. *Inorg. Chim. Acta* **1988**, *141*, 167−168.
(100) Nyholm, R. S.; Turco, A. *Chem. Ind. (London)* **1960**, 74.
(101) Cooper, S. R.; Calvin, M. *J. Am. Chem. Soc.* **1977**, *99*, 6623−6630.
(102) Collins, M. A.; Hodgson, D. J.; Michelsen, K.; Towle, D. K. *J. Chem. Soc., Chem. Commun.* **1987**, 1659−1660.
(103) Wieghardt, K.; Bossek, U.; Zsolnai, L.; Huttner, G.; Blondin, G.; Girerd, J.-J.; Babonneau, F. *J. Chem. Soc., Chem. Commun.* **1987**, 651−653.
(104) Philouze, C.; Blondin, G.; Girerd, J.-J.; Guilhem, J.; Parcard, C.; Lexa, D. *J. Am. Chem. Soc.* **1994**, *116*, 8557−8565.

complexes has been identified with χ_0. Substitution of the activation energy, $\Delta G^*_{loc} = \chi_0/4 = 2658\ cm^{-1}$, and the *f* factor, 0.56, into eq 16a yields the ratio $k/k_{loc} = 269$ for the rate constants for the self-exchange reactions of the partially delocalized bispicen complex and the localized tmpa complex. Of course, the excellent agreement with the experimental value, $k/k_{loc} = 260$,[58] is rather fortuitous if one considers the simplifications made in the derivation. Nonetheless, this result confirms the idea that intramolecular electron delocalization influences the rate of intermolecular electron transfer.

In future studies, we intend to analyze a wider class of donor−acceptor systems, including exchange-coupled acceptor molecules and tri- and tetranuclear clusters. In addition, intramolecular relaxation over the spin levels in these clusters, possibly needed in preventing the return of the excited-state electron to the donor site and in reestablishing the excited-state populations after electron transfer, will be considered. Electronic structure analysis of the molecular origin of the stronger interaction between the manganese sites in the bispicen complex, as compared to the tmpa complex, may give additional insight into the intrinsic electronic factors which determine electron-transfer kinetics.

5. Conclusions

The main conclusions of this theoretical study of electron transfer from exchange-coupled polynuclear clusters can be summarized as follows:

1. The activation energy for self-exchange reactions between clusters is reduced by intramolecular electron delocalization (eq 11). This reduction leads to an increase in the rate constant for electron transfer (eq 16). The theory reproduces the trend observed in the relative magnitudes of the rate constants measured for the self-exchange reactions in a series of binuclear manganese compounds with variable degrees of electron delocalization.

2. Excited states in the spin ladders of clusters can be major contributors to electron transfer. In particular, these contributions become important when the activation energy for electron transfer from the ground state is big and the barrier minima for the excited states are dispersed over a broad redox potential range as a result of double-exchange interaction (Figure 5). Electron transfer via excited states can considerably accelerate the transfer at potentials where the reaction would otherwise be negligibly slow.

3. Spin-selection rules are an important factor in electron-transfer reactions involving exchange-coupled clusters. In the presence of double exchange, variations in HDvV exchange can tune the rate constant (Figure 6). This observation suggests that a cluster can act as a molecular switch for exchange-controlled electron gating.

This study indicates that HDvV exchange and double exchange are important determinants of the kinetics of electron transfer, especially when these interactions are strong, such as in Fe−S clusters.

Acknowledgment. This research was supported by the National Institutes of Health Grant GM 22701 and the National Science Foundation Grant MCB-9406224 to E.M.

IC961298Q